Thermal modelling and analysis of an oil-free linear compressor

M J Oliveira, M C Diniz and C J Deschamps[1]
POLO Research Labs for Emerging Technologies in Cooling and Thermophysics
Federal University of Santa Catarina, 88040-900, Florianopolis, SC, Brazil

E-mail: deschamps@polo.ufsc.br

Abstract. Gas superheating in the suction system may significantly reduce the volumetric and isentropic efficiencies of small reciprocating compressors adopted for household refrigeration. This paper reports a thermal modelling approach developed to predict superheating in an oil-free linear compressor. A simulation code based on the finite volume method was adopted to solve heat conduction in the solid components and gas flow inside the compressor shell. In order to reduce the computational cost, the compression cycle inside the cylinder was modelled with a transient lumped formulation, but in a coupled manner with the remainder of the solution domain. Comparisons between numerical and experimental results of temperature showed discrepancies in some solid components and in the gas path along the discharge system. However, the model was able to predict suction gas superheating in good agreement with measurements. A sensitivity analysis of the temperature distribution with respect to two design parameters was also carried out. The model is particularly useful for compressor design since no experimental calibration is required.

1. Introduction

Linear compressors work through the reciprocating motion of a piston provided by the combination of a linear motor and a spring [1]. This type of actuating mechanism significantly reduces the number of moving parts, increasing the mechanical efficiency and making the compressor suitable for miniaturization [2] and electronic cooling applications [3]. Most of current studies on compressor technology aim to increase the thermodynamic efficiency. An aspect that acts to reduce the volumetric and isentropic efficiencies of hermetic compressors is gas superheating due to heat transfer between internal components [4].

Heat transfer in reciprocating compressors has been extensively studied with different numerical approaches, following lumped, differential and hybrid formulations. Lumped models [5-8] are used when low computational cost is required in the first phases of compressor design. Differential models are necessary when full description of the phenomenon is needed [9-11]. Hybrid models [12-14] combine lumped and differential formulations and offer a trade-off between computational cost and accuracy.

Schreiner [15] carried out a comparative analysis between differential and hybrid models to predict the temperature distribution of a reciprocating compressor. The author observed that predictions of the hybrid model were in better agreement with experimental data. The discrepancies observed in the

[1] To whom any correspondence should be addressed.

differential model were attributed to the flow of lubricating oil over the compressor components, which was not considered in the simulation. The hybrid model takes this into account through experimental calibration of thermal conductances.

This paper presents a model to predict the temperature field of an oil-free linear reciprocating compressor, with especial attention to the gas superheating during the suction process. The simulation approach consists of two coupled submodels: a transient lumped model for the compression cycle and a finite volume model for heat transfer in solids components and in the gas flow inside the compressor.

2. Simulation model

2.1. Compression cycle

The compression cycle is modelled with a transient lumped formulation [8] via four groups of equations: (i) equations to describe the variation of the compression chamber volume; (ii) equations for mass and energy balances inside the compression chamber; (iii) equations for valve dynamics; (iv) equations to estimate the mass flow rate through valves and leakage through the piston-cylinder gap. The model allows predictions for discharge temperature in the discharge orifice, compression power and mass flow rate.

The motion of the piston as a function of time is described by:

$$x_{pis}(t) = -\omega A \sin(2\pi f t) \tag{1}$$

where f is the operating frequency, A is the motion amplitude and ω is an amplitude factor that is adjusted between 0.85 and 1 to match the input data of power consumption. It should be noted that x_{pis} is referenced to the mid-stroke position, with x_{pis}= -ωA when the piston is at top dead centre and x_{pis}= +ωA when the piston is at bottom dead centre.

The instantaneous volume of the compression chamber is given by:

$$\forall_{cyl}(t) = \forall_{\delta,geo} + \{h_o + \omega A + x_{pis}(t)\} A_{pis} \tag{2}$$

where the first term is related to the geometric dead volume. In the second term, A_{pis} and h_o are the area of the head of the piston and minimum height of the compressor chamber, respectively.

The thermodynamic properties of the gas in the compression chamber are evaluated via a transient lumped formulation of the conservation equations. After some mathematical manipulations of the energy equation, the equation to evaluate the temperature of the gas, $T_G(t)$, is given by:

$$\frac{dT_G}{dt} = M - NT_G \tag{3}$$

where

$$M = \frac{1}{m_G c_v}\left[H_G A_w T_w - h_G \frac{dm_G}{dt} + (\dot{m}_{sv} h_{sv}) - (\dot{m}_{dv} h_{dv}) - (\dot{m}_{leak} h_{leak})\right] \tag{4}$$

$$N = \frac{1}{m_G c_v}\left[H_G A_w + \left.\frac{\partial p_G}{\partial T_G}\right|_v \frac{d\forall_G}{dt} - \left.\frac{\partial p_G}{\partial T_G}\right|_v v_G \frac{dm_G}{dt}\right] \tag{5}$$

In the above equations, H_G is the convective heat transfer coefficient required to estimate the instantaneous heat exchange between the gas and the cylinder wall, which was obtained from the correlation proposed by [16], c_v is the specific heat coefficient and v_G is the specific volume of the gas. The instantaneous volume of the compression chamber is obtained from equation (2) and the mass of gas inside the compression chamber, m_G, allows the determination of the gas density. The

instantaneous gas pressure, p_G, is obtained by introducing the gas density and temperature in a state equation.

The instantaneous compression power is given by

$$\dot{W} = -f \int p_G d\forall_{cyl} \tag{6}$$

The simulation of the compression cycle requires estimates for the temperatures of the gas in the suction chamber ($T_{suc,o}$) and of the cylinder wall (T_w). The method used for this purpose will be explained shortly.

Linear compressors adopt reed type valves that open and close under changing pressure on each face. Valve dynamics is represented by a one degree of freedom mass-spring model:

$$M_v \ddot{x}_v + c_v \dot{x}_v + K_v x_v = F_v \tag{7}$$

where M_v, c_v and K_v are the reed equivalent mass, damping coefficient and stiffness, respectively. In equation (7), x, $\dot{x}$ and $\ddot{x}$ are the instantaneous reed lift, velocity and acceleration, respectively. The force F_v, resulting from the pressure load on the reed is obtained with reference to the effective force area, A_{ef}, which is determined numerically or experimentally from the pressure difference across the valve, Δ_{pv}, according to $A_{ef} = F_v / \Delta_{pv}$ [17]. The effective force area can be understood as a parameter related to how efficiently the pressure difference Δ_{pv} opens the valve. The differential equation for the valve dynamics, equation (7), was solved using an explicit Euler method.

The mass flow rate through the valve, $\dot{m}_v$, is evaluated with reference to the isentropic flow condition and the concept of effective flow area, A_{ee}, which accounts for viscous effects. Therefore,

$$\dot{m}_v = A_{ee} p_{up} \sqrt{\frac{2k}{(k-1)RT_{up}} \left[R_p^{2/k} - R_p^{(k+1)/k} \right]} \tag{8}$$

where p_{up} and T_{up} denote pressure and temperature upstream, k is the specific heat ratio, R is the refrigerant gas constant and R_p is the pressure ratio between the cylinder and discharge/suction chamber. Naturally, values for p_{up}, T_{up} and R_p vary along the compression cycle, whether the flow is critical or sub critical, and also with flow direction.

Gas leakage through the piston-cylinder gap was modelled employing a Couette-Poiseuille flow model [18].

2.2. Fluid flow and heat transfer inside the compressor

A commercial code (Ansys FLUENT v.14) based on the finite volume method was employed to predict heat transfer in solid components and along the gas path in the suction system, internal environment and discharge system. The system of governing equations is formed by the conservation equations for mass, momentum and thermal energy. The turbulent flow that prevails inside the compressor was solved with the concept of Reynolds-averaged quantities through the SST model.

A second-order upwind scheme was adopted to interpolate the flow quantities needed at the control volume faces. The coupling between the pressure and velocity fields was achieved with the SIMPLE algorithm [19]. The system of algebraic equations was solved with a segregated implicit algorithm.

The simulation model is prepared following three steps: (i) simplifications of the compressor geometry for mesh generation, (ii) specification of boundary conditions and (iii) simulation of fluid flow and heat transfer in a coupled manner with the lumped model for the compression chamber (section 2.1).

The solution domain of the differential model includes the suction and discharge systems, region inside the compressor shell and solid components. Especial care was taken to properly discretize regions of high gradients, such as near solid walls. The mesh for the solid and fluid solution domains had nearly 17 million tetrahedral and prismatic volumes. When it was imported to the solver, the number of volumes was reduced to around 7 million, with agglutination of tetrahedral volumes in the form of polyhedral volumes.

Boundary conditions are required to characterize the compressor operating condition and to ensure the coupling between the lumped and differential models. Figure 1 presents the compressor solution domain of the differential model, identifying different boundaries ($\mathcal{C}$). The volume ($\mathcal{V}_1$) of the linear motor coils was modelled as a heat source $\dot{Q}_{mot}$, which was estimated from the electrical motor efficiency. On the other hand, figure 2 illustrates the compression chamber where the lumped model is applied; hence there is no mesh inside it. In figure 2, it is also possible to identify the boundaries $\mathcal{C}_4$, $\mathcal{C}_5$ and $\mathcal{C}_6$ that exchange information between the lumped and differential models.

Evaporating and condensing pressures were imposed as boundary conditions for the inlet ($\mathcal{C}_1$) and outlet ($\mathcal{C}_2$), respectively. The inlet temperature was measured in the calorimeter (T_{in} = 32ºC). The ambient temperature and the convective heat transfer coefficient on the compressor shell external surface were T_{amb} = 32ºC and h_{amb} = 20W/m^{2}K, respectively.

Table 1 and table 2 present the variables related to each boundary ($\mathcal{C}$) and the volume ($\mathcal{V}_1$), as well as the source from which one is obtained: input data or from exchange of information between the lumped and differential models.

3. Solution procedure

The lumped and differential models are solved in a coupled manner until convergence is achieved, when the temperature field of the compressor is established. The lumped model is called inside the finite volume solver every four iterations.

The convergence of the solution procedure was verified by monitoring six global parameters: i) temperature of the gas at the suction orifice $\mathcal{C}_5$ ($T_{suc,o}$) ii) temperature at the cylinder wall $\mathcal{C}_4$ (T_w); iii) overall energy balance in the fluid flow domain; iv) heat transfer at the cylinder wall $\mathcal{C}_4$; v) mass flow rate at the compressor inlet $\mathcal{C}_1$ ($\dot{m}_{in}$); vi) mass flow rate at the compressor outlet $\mathcal{C}_2$ ($\dot{m}_{out}$). The convergence criterion for these global parameters is expressed as follows:

$$\frac{|\phi - \bar{\phi}|}{SF} < 10^{-3} \tag{9}$$

In equation (9), ϕ represents the global parameter being analysed and $\bar{\phi}$ is the average value of ϕ in the last ten most recent iterations. The denominator SF in equation (9) varies according to the global parameter ϕ of interest. Accordingly, $SF = T_{dis,o} - T_{in}$ when ϕ represents temperature; $SF = \dot{m}_{suc,o}$ when ϕ is mass flow rate and $SF = \dot{W}$ when ϕ is either energy balance or heat transfer.

In addition to monitoring the convergence of global parameters, the solution of the governing equations in the differential model was also verified for convergence by examining scaled residuals, as defined in [20]. The solution procedure of the governing equations for mass, momentum and turbulence was considered to be converged when their residuals were smaller than 10^{-3}, whereas a residual of 10^{-6} was used for the energy equation. The simulation was concluded when the convergence criteria for the six global parameters and differential model were simultaneously satisfied.

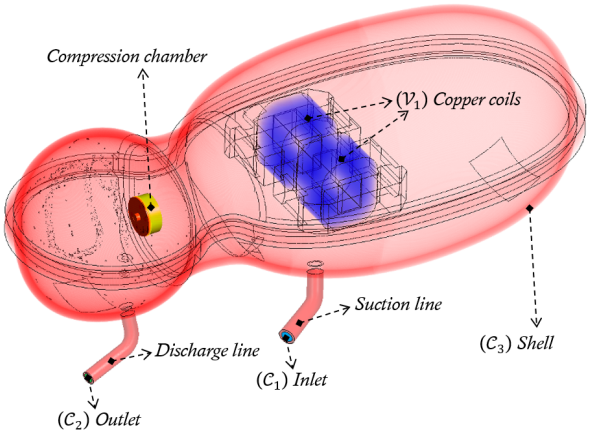

Figure 1. Boundaries of the compressor solution domain.

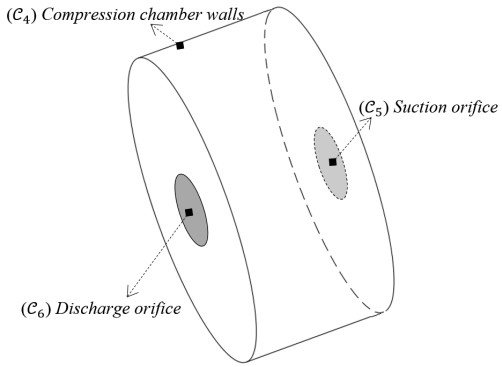

Figure 2. Boundaries of the compression chamber domain.

Table 1 and table 2 assigned each boundary ($\mathcal{C}$, $\mathcal{V}_1$), presented in figure 1 and figure 2, to a boundary condition necessary to create the coupling of lumped and differential models. In this way, an interactive loop is built (cycle) until the convergence, when the thermal profile of the linear compressor is found.

By following this solution procedure, about 1000 cycles were required to establish convergence, with a processing time of approximately 6 minutes per cycle on a computer with an Intel i7 3.2 GHz processor and 64 GB of RAM. As a comparison, the processing time of a complete simulation with hybrid models [13-15] is of order of minutes.

Table 1. Boundary and heat generation conditions of the differential model.

Boundary	Boundary conditions	Source
Inlet $\mathcal{C}_1$	p_{in}, T_{in}	Input data
Outlet $\mathcal{C}_2$	p_{out}	Input data
Compressor shell $\mathcal{C}_3$	h_{amb}, T_{amb}	Input data
Compression chamber walls $\mathcal{C}_4$	$\dot{Q}_w$	Lumped model
Suction orifice $\mathcal{C}_5$	$\dot{m}_{suc,o}$	Lumped model
Discharge orifice $\mathcal{C}_6$	$\dot{m}_{dis,o}$, $T_{dis,o}$	Lumped model
Copper coils $\mathcal{V}_1$	$\dot{Q}_{mot}$	Lumped model

Table 2. Boundary conditions of the lumped model.

Boundary	Boundary condition	Source
Compression chamber walls $\mathcal{C}_4$	T_w	Differential model
Suction orifice $\mathcal{C}_5$	$T_{suc,o}$	Differential model

4. Results

Simulations were carried out for a 120 Hz linear compressor, operating with R134a under evaporating temperature T_e = -23.3ºC and condensing temperature T_c = 40.5ºC. Accordingly, boundary conditions of pressure and temperature at the inlet were 115kPa and 305K, respectively. The compressor geometric dimensions are typical of small reciprocating compressors used for domestic refrigeration.

The numerical results were validated through comparisons with experimental data of temperature at different locations in the gas path (figure 3) and solid components (figure 4). Figure 5 shows the deviations between predictions and measurements of temperatures (ΔT) for points **A** to **J** identified in figure 3 along the gas path inside the compressor. As can be seen, there is reasonable agreement

between both results, especially from point **A** to **F**, which represents the suction gas superheating. The only discrepancy occurs at point **H** located inside the discharge chamber, with a difference of approximately 17ºC. Figure 6 presents the comparison between numerical and experimental results for the compressor solid components. As can be seen, there are considerable differences at points **R** and **S**, as well as at points **T** and **U** on the compressor shell surface.

The discrepancies observed in figures 5 and 6 may occur in part because the model neglects the motion of the mechanical kit inside the compressor. A dynamic mesh could be used to allow the modelling of this mechanism of convection intensification, but would result in a much more complex simulation model and higher computational cost. Since heat transfer inside the compressor is numerically solved, the difference between predictions and measurements may also be associated with truncation error due to inadequate grid discretization. This aspect will be further analysed in future work.

After validation, the model was applied to analyse the temperature distribution sensitivity in relation to two parameters: (i) convective heat transfer coefficient on the compressor external surface, h_{amb}, whose reference value is 20W/m^{2}K; (ii) thermal conductance of the insulating gasket (k/l), which is positioned immediately above positions **Q** and **R** (figure 4) to reduce heat transfer through conduction from the discharge system to the suction system. The conductance of the insulation gasket (k/l) was varied by specifying two thermal conductivities (k = 0.1 and 0.3 W/m K) different from the reference value (k = 0.2W/m K), but keeping its thickness (l) constant and considering h_{amb} = 15W/m²K. Figures 7 and 8 show the temperature variations (ΔT) observed along the gas path due the aforementioned modifications in h_{amb} and k.

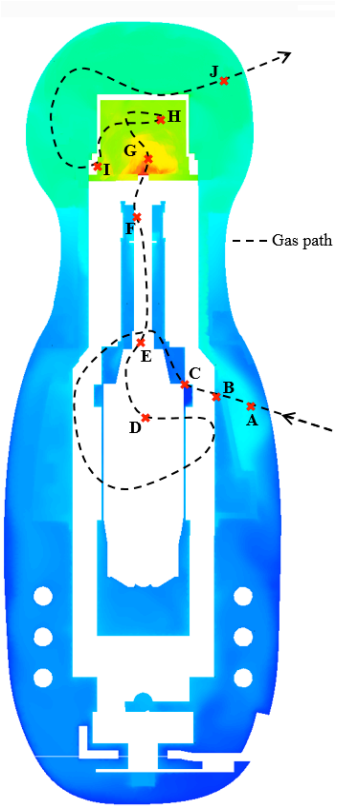

Figure 3. Temperature field of gas domain in the baseline condition (solid domain hidden).

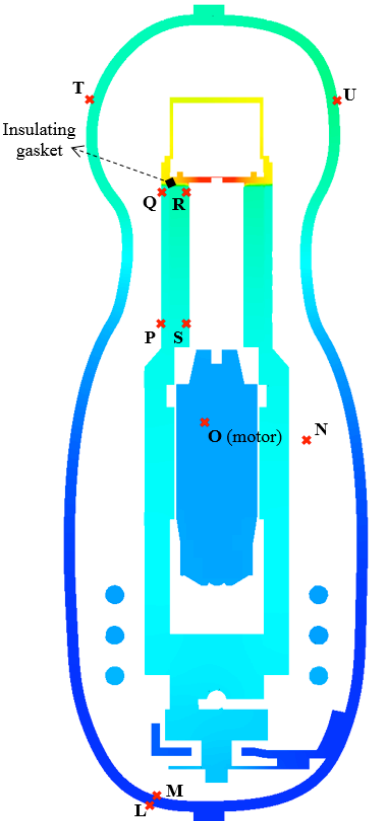

Figure 4. Temperature field of solid domain in the baseline condition (gas domain hidden).

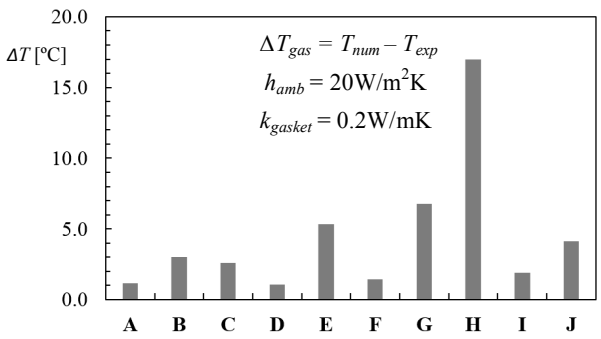

Figure 5. Differences between predictions and measurements of temperature along the gas path.

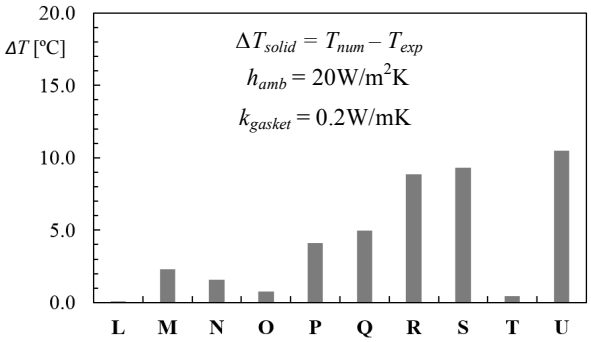

Figure 6. Differences between predictions and measurements of temperature in the solid components.

As expected, figure 7 shows a considerable increase of temperature when the convective heat transfer coefficient is reduced from its reference value (20W/m²K). On the other hand, the compressor thermal profile is much less dependent on the insulating gasket conductance (figure 8). Nevertheless, point **F** (figure 3) corresponds to the position where the gas is suctioned into the compression chamber and, therefore, the temperature there affects the compressor isentropic and volumetric efficiencies. The model predicts an increase of 4ºC when the thermal conductivity is varied from 0.1W/mK to 0.3W/mK.

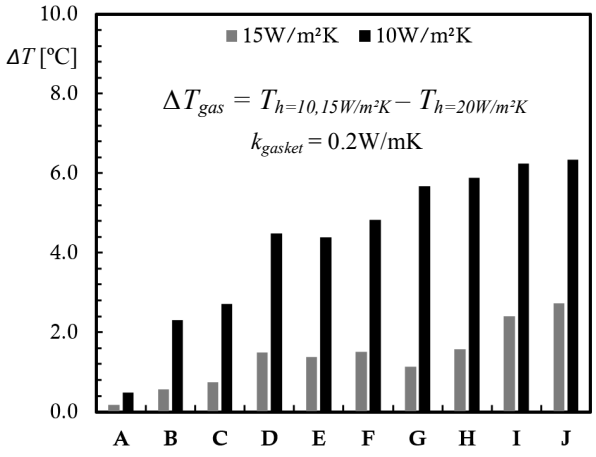

Figure 7. Effect of the external convective heat transfer coefficient on the temperature field (reference: h_{amb} = 20W/m²K).

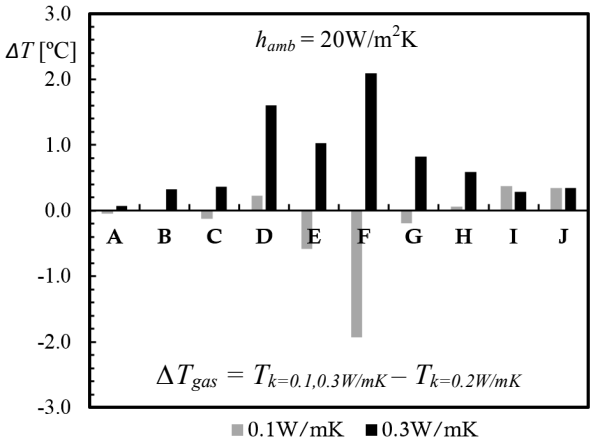

Figure 8. Effect of the insulating gasket thermal conductivity k on the temperature field (reference: k = 0.2W/mK).

5. Conclusions

A simulation model was developed and applied to predict the temperature distribution of an oil-free linear compressor designed for household refrigeration. The model adopts a lumped formulation for the compression cycle and a differential formulation for fluid flow and heat transfer in the remainder components of the compressor. Predictions and experimental data were found in reasonable agreement, with the exception of some locations in the gas path and solid components. The model was applied to analyse the influence of the external convection heat transfer and insulating gasket on suction superheating. The model is particularly useful for compressor design since it does not require experimental calibration.

Acknowledgments
The present study was developed as part of a technical-scientific cooperation program between the Federal University of Santa Catarina and EMBRACO. The authors also acknowledge the support provided by EMBRACO and CNPq (Brazilian Research Council) through Grant No. 573581/2008-8 (National institute of Science and Technology in Refrigeration and Thermophysics) and CAPES (Coordination for the Improvement of High Level Personnel).

References
[1] Van Der Walt N and Unger R 1994 Linear Compressors – A Maturing Technology *Proc. Int. Compressor Eng. Conf. at Purdue (West Lafayette, IN, USA)*
[2] Bradshaw C, Groll E and Garimella S 2011 A Comprehensive Model of a Miniature-Scale Linear Compressor for Electronics Cooling *Int. J. Refrigeration* **34** 63–73
[3] Unger, R L and Novotny S 2002 A High Performance Linear Compressor for CPU Cooling *Proc. Int. Compressor Eng. Conf. at Purdue (West Lafayette, IN, USA)*
[4] Prasad B G S 1998 Heat transfer in Reciprocating Compressors *Proc. Int. Compressor Eng. Conf. at Purdue (West Lafayette, IN, USA)*
[5] Meyer W and Thompson H 1988 An Analytical Model of Heat Transfer to the Suction Gas in a Low-Side Hermetic Refrigeration Compressor *Proc. Int. Compressor Eng. Conf. at Purdue (West Lafayette, IN, USA)*
[6] Ooi K T 2003 Heat Transfer Study of a Hermetic Refrigeration Compressor *J. Applied Thermal Engineering* **23** 1931–45
[7] Padhy S K 1992 Heat Transfer Model of a Rotary Compressor *Proc. Int. Compressor Eng. Conf. at Purdue (West Lafayette, IN, USA)*
[8] Todescat M L, Fagotti F, Ferreira R T S and Prata A T 1992 Thermal Energy Analysis in Reciprocating Hermetic Compressors *Proc. Int. Compressor Eng. Conf. at Purdue (West Lafayette, IN, USA)*
[9] Birari Y V, Gosavi S S and Jorwekar P P 2006 Use of CFD in Design and Development of R404a Reciprocating Compressor *Proc. Int. Compressor Eng. Conf. at Purdue (West Lafayette, IN, USA)*
[10] Chikurde C and Longanathan E 2002 Thermal Mapping of Hermetically Sealed Compressors Using Computational Fluid Dynamics Technique *Proc. Compressor Eng. Conf. at Purdue (West Lafayette, IN, USA)*
[11] Raja B, Seckar S J, Lal D M and Kalanidhi A 2003 A Numerical Model for Thermal Mapping in a Hermetically Sealed Reciprocating Compressor *Int. J. Refrigeration* **26** 652–58
[12] Almbauer R A, Burgstaller A, Abidin Z and Nagy D 2006 3-Dimensional Simulation for Obtaining the Heat Transfer Correlations of a Thermal Network Calculation for the Hermetic Reciprocating Compressors *Proc. Int. Compressor Eng. Conf. at Purdue (West Lafayette, IN, USA)*
[13] Ribas Jr F A 2007 Thermal Analysis of Reciprocating Compressors *Proc. Int. Conf. on Compressors and their Systems (London, UK)*
[14] Sanvezzo Jr J and Deschamps C J 2012 A Heat Transfer Model Combining Differential and Integral Formulations for Thermal Analysis of Reciprocating Compressors *Proc. Int. Compressor Eng. Conf. at Purdue (West Lafayette, IN, USA)*
[15] Schreiner J E 2008 Simulation Methodologies Development for Thermal Management Solution Analysis Applied to Refrigeration Reciprocating Compressor *MSc Dissertation (Federal University of Santa Catarina, Florianopolis, Brazil)*
[16] Annand W J D 1963 Heat Transfer in the Cylinders of the Reciprocating Internal Combustion Engines *Proc. Institution of Mechanical Engineers* **177** 973–96
[17] Deschamps C J, Prata A T and Ferreira R T S 2000 Modelling of Turbulent Flow Through Radial Diffusers *J. Brazilian Society of Mechanical Sciences* **22** 31–41

[18] Ferreira R T S and Lilie D E B 1984 Evaluation of the Leakage Through the Clearance Between Piston and Cylinder in Hermetic Compressor *Proc. Int. Compressor Eng. Conf. at Purdue (West Lafayette, IN, USA)*
[19] Patankar S V 1980 *Numeric Heat Transfer and Fluid Flow* (New York: Hemisphere Publishing)
[20] ANSYS Inc. 2014 *FLUENT User's Guide* (Lebanon/NH, USA)